

This is the accepted manuscript made available via CHORUS. The article has been published as:

Upper critical fields and two-band superconductivity in  
 $\text{Sr}_{1-x}\text{Eu}_x(\text{Fe}_{0.89}\text{Co}_{0.11})_2\text{As}_2$   
( $x=0.20$  and  $0.46$ )

Rongwei Hu, Eun Deok Mun, M. M. Altarawneh, C. H. Mielke, V. S. Zapf, S. L. Bud'ko, and  
P. C. Canfield

Phys. Rev. B **85**, 064511 — Published 13 February 2012

DOI: [10.1103/PhysRevB.85.064511](https://doi.org/10.1103/PhysRevB.85.064511)

# Upper critical fields and two-band superconductivity in $\text{Sr}_{1-x}\text{Eu}_x(\text{Fe}_{0.89}\text{Co}_{0.11})_2\text{As}_2$ ( $x = 0.20$ and $0.46$ )

Rongwei Hu<sup>1,\*</sup>, Eun Deok Mun<sup>2</sup>, M. M. Altarawneh<sup>2,†</sup>, C. H. Mielke<sup>2</sup>, V. S. Zapf<sup>2</sup>, S. L. Bud'ko<sup>1</sup>, P. C. Canfield<sup>1</sup>

<sup>1</sup>*Ames Laboratory, U.S. DOE and Department of Physics and Astronomy,  
Iowa State University, Ames, IA 50011, USA and*

<sup>2</sup>*National High Magnetic Field Laboratory, Los Alamos National Laboratory, Los Alamos, New Mexico 87545, USA*

(Dated: January 25, 2012)

The upper critical fields,  $H_{c2}(T)$  of single crystals of  $\text{Sr}_{1-x}\text{Eu}_x(\text{Fe}_{0.89}\text{Co}_{0.11})_2\text{As}_2$  ( $x = 0.20$  and  $0.46$ ) were determined by radio frequency penetration depth measurements in pulsed magnetic fields.  $H_{c2}(T)$  approaches the Pauli limiting field but shows an upward curvature with an enhancement from the orbital limited field as inferred from Werthamer-Helfand-Hohenberg theory. We discuss the temperature dependence of the upper critical fields and the decreasing anisotropy using a two-band BCS model.

PACS numbers: 74.25.Dw, 74.25.Op, 74.70.Dd

## I. INTRODUCTION

The upper critical field  $H_{c2}(T)$  and its anisotropy are fundamental characteristics of a type-II superconductor, they provide information about the underlying electronic structure and can shed light on the mechanism of Cooper pair breaking. Therefore both for the understanding of superconductivity as well as potential application, extensive studies of  $H_{c2}(T)$  have been performed on the recently discovered FeAs-based superconductors. Large upper critical fields have been observed for FeAs superconductors.<sup>1–7</sup> More interestingly, some of their  $H_{c2}(T)$  exhibit pronounced upward curvature of  $H_{c2}(T)$ , implying a multiband nature of superconductivity.<sup>5,8–10</sup> In contrast to the high  $T_c$  cuprates with their very large anisotropy, measurements of  $H_{c2}(T)$  of the FeAs superconductors have revealed that the anisotropic ratio  $\gamma = H_{c2}^{ab}/H_{c2}^c$  decreases with decreasing temperature and becomes nearly isotropic at low temperatures for the 122 and 111 type of FeAs materials.<sup>6–8,11</sup>

Previous study of Eu doped  $\text{Sr}(\text{Fe}_{0.88}\text{Co}_{0.12})_2\text{As}_2$  demonstrated the interaction between the FeAs-based superconductivity and magnetism due to  $\text{Eu}^{2+}$ : in the disordered paramagnetic region of  $\text{Eu}^{2+}$ , superconductivity is weakly suppressed by spin-flip scattering associated with the local magnetic moments of  $\text{Eu}^{2+}$ ; it is further suppressed with developing long range antiferromagnetic order of  $\text{Eu}^{2+}$  and coexists with antiferromagnetism of  $\text{Eu}^{2+}$  as long as  $T_c > T_N$ .<sup>12</sup> It is of great interest to see how the superconductivity is affected by the magnetism of  $\text{Eu}^{2+}$  by mapping out the  $H - T$  phase diagram.

Moreover, in the study of the interplay of superconductivity and magnetism, it is proposed by Jaccarino and Peter<sup>13</sup> that for certain rare earth bearing intermetallics the external magnetic field, which in general inhibits superconductivity, may be cancelled by the effective exchange field  $H_{eff}$  of the magnetic moments, imposed on the conduction electrons, when  $H_{eff}$  is opposite to the direction of applied field. Therefore superconductivity can occur in two domains, one at low field, where pair-breaking field is still small, and one

at high field in the compensation region. Experimentally, an anomalous enhancement of  $H_{c2}(T)$  was first reported by Fischer *et al*<sup>14</sup> in  $\text{Sn}_{1.2(1-x)}\text{Eu}_x\text{Mo}_{6.35}\text{S}_8$  and  $\text{Pb}_{1-x}\text{Eu}_x\text{Mo}_{6.35}\text{S}_8$  chevre phases. Attributed to this "Jaccarino-Peter" effect, magnetic field induced superconductivity in the  $H_{c2} - T$  phase diagram was indeed observed in  $\text{Eu}_{0.75}\text{Sn}_{0.25}\text{Mo}_6\text{S}_{7.2}\text{Se}_{0.8}$  and fitted well with the Jaccarino-Peter scenario.<sup>15</sup> Therefore, the properties of  $\text{Sr}_{1-x}\text{Eu}_x(\text{Fe}_{0.89}\text{Co}_{0.11})_2\text{As}_2$ , as possible candidates for observation of Jaccarino-Peter effect, are worth investigating.

In this paper we report the upper critical fields of  $\text{Sr}_{1-x}\text{Eu}_x(\text{Fe}_{0.89}\text{Co}_{0.11})_2\text{As}_2$  ( $x = 0.20$  and  $0.46$ ) single crystals determined by radio frequency contactless penetration depth measurements. The two selected samples are the representative concentrations in the disordered paramagnetic region and coexistence region of superconductivity and antiferromagnetism. We find that for both concentrations the curves of  $H_{c2}(T)$  can be consistently explained by the two-band model and the anisotropy decreases with temperature approaching an isotropic state at low temperatures.

## II. EXPERIMENT

Single crystals of  $\text{Sr}_{1-x}\text{Eu}_x(\text{Fe}_{0.89}\text{Co}_{0.11})_2\text{As}_2$  were grown from self flux, similar to that in Ref. 12. But the annealing procedure is different from the previous one. After FeAs flux was decanted, sample ampules were annealed at 500 °C for 24 hours before opening. Thus the air exposure of the crystals was minimized. Chemical composition was determined by wavelength dispersive x-ray spectroscopy (WDS) in a JEOL JXA-8200 electron microscope. Magnetic susceptibility was measured in a Quantum Design MPMS. The temperature and magnetic field dependences of the electrical resistance were measured using the four probe ac ( $f = 16\text{Hz}$ ) technique in a Quantum Design PPMS. Radio frequency (rf) contactless penetration depth measurements were performed on the single-crystal sample in a 60 T pulsed field magnet

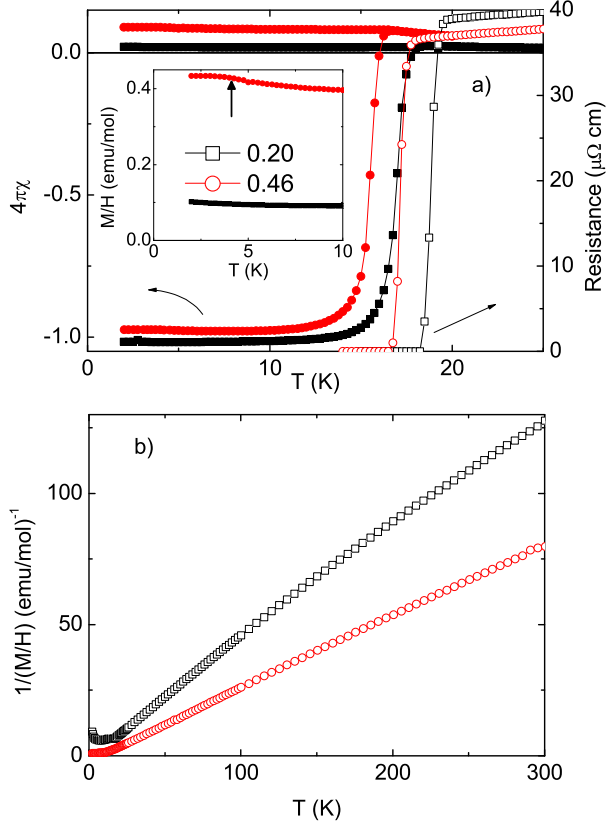


FIG. 1: a) Low temperature magnetic susceptibility measured in a magnetic field of 100 Oe applied in  $ab$  plane and resistivity in zero field. Inset shows an expanded view of the field-cooled curve. The arrow indicates the antiferromagnetic transition. b) Inverse in-plane magnetic susceptibility measured in 10 kOe.

with a 10 ms rise time and a 40 ms extended decay. The rf technique is highly sensitive to small changes ( $\sim 1$ –5 nm) in the rf penetration depth, thus it is an accurate method for determining the upper critical field in anisotropic superconductors.<sup>16</sup> Small single crystals were selected because of the eddy current heating in pulsed field. To determine the upper critical-field anisotropy, the single crystal was measured in two,  $H \parallel ab$  and  $H \parallel c$ , configurations. More details about this technique can be found in Ref.4, 17, 18.

### III. RESULTS AND DISCUSSIONS

The actual compositions of the two samples determined by WDS were  $\text{Sr}_{0.797}\text{Eu}_{0.203}(\text{Fe}_{0.888}\text{Co}_{0.112})_2\text{As}_2$  and  $\text{Sr}_{0.537}\text{Eu}_{0.463}(\text{Fe}_{0.885}\text{Co}_{0.115})_2\text{As}_2$ . For brevity, we denote them as Eu20 and Eu46 sample in the following text. The Co concentrations are close to the optimal doping,  $x \sim 0.12$ , for  $\text{Sr}(\text{Fe}_{1-x}\text{Co}_x)_2\text{As}_2$  as in Ref. 12.

Figure 1(a) shows the low temperature magnetic susceptibility and resistivity of the two samples. Since we are measuring the in-plane magnetic susceptibility and the sample is thin plate-like, with aspect ratio (in-plane dimension/thickness) of more than 10, the demagnetization factor is negligibly small (less than 0.05).<sup>19</sup> The large diamagnetic shielding indicates bulk superconductivity. The superconducting transition temperatures inferred from the first deviation point from the normal magnetic susceptibility of the zero-field-cool curve are 18 K and 16.2 K for Eu20 and Eu46 respectively. The Eu46 sample shows a weak anomaly due to antiferromagnetic ordering of  $\text{Eu}^{2+}$  at 3.5 K as indicated in the inset of Fig. 1(a) as that in Ref. 12. The  $T_c$  in resistivity as inferred from by extrapolating the steepest slope to zero resistance are 18.3 K and 16.8 K for the two samples, in agreement with the magnetic susceptibility measurements. The inverse in-plane magnetic susceptibility measured in 10 kOe of the two samples is plotted in Fig.1 (b). The Curie-Weiss fits above 150 K give an estimated Eu concentration of 0.22 and 0.47 by assuming  $7.94 \mu_B/\text{Eu}^{2+}$  ion. Thus all the above observations are consistent with those in Ref. 12 and show that Eu20 is in the disordered paramagnetic region of  $\text{Eu}^{2+}$  and Eu46 is in the coexistence region of superconductivity and antiferromagnetism. This being said, we should note that the  $T_c$  values of the present samples are 6–7 K higher than those in Ref. 12. This is most likely due to the difference in heat treatment and also may be due to slight shift in Co concentrations. Fortunately, given robust nature of  $\text{Eu}^{2+}$  magnetism, this shift in  $T_c$  does not adversely effect our goal of studying effects of local moment magnetism on  $H_{c2}(T)$ .

The frequency shift as a function of magnetic field applied parallel and perpendicular to the  $ab$  plane at different temperatures from 1.5 to 19 K for Eu20 is shown in Fig. 2. The normal state has a smooth and nearly linear field dependence as manifested by the 19 K curve.<sup>20</sup>  $H_{c2}$  is identified as the point at which the slope of the  $\Delta F$  intercepts the normal state background of 19 K. Other criterion, e.g. first point deviating from the normal state background can be used and the difference between these two criteria is taken as the error bar for  $H_{c2}(T)$ . For  $H \parallel c$  in Fig. 2(b), the sample has a weaker coupling to the detection coil, resulting in a smaller but still easily resolvable frequency shift. The same rf measurements are performed on Eu46 sample for both orientations for temperatures down to 0.51 K and shown in Fig. 3. In the previous study in Ref. 12, it was shown that the  $\text{Eu}^{2+}$  moments undergo a metamagnetic transition from antiferromagnetic to ferromagnetic above a magnetic field of 4 kOe. Thus it behaves as a superconductor with ferromagnetically coupled  $\text{Eu}^{2+}$  moments at low temperature high field. In order to look for possible Jaccarino-Peter effect, the frequency shift of Eu46 sample was measured in field up to 60 T at the base temperature 0.51 K for both directions (inset in Fig. 3(b)). No anomaly associated with superconductivity can be observed in high fields. So either the magnetic field is still too low to

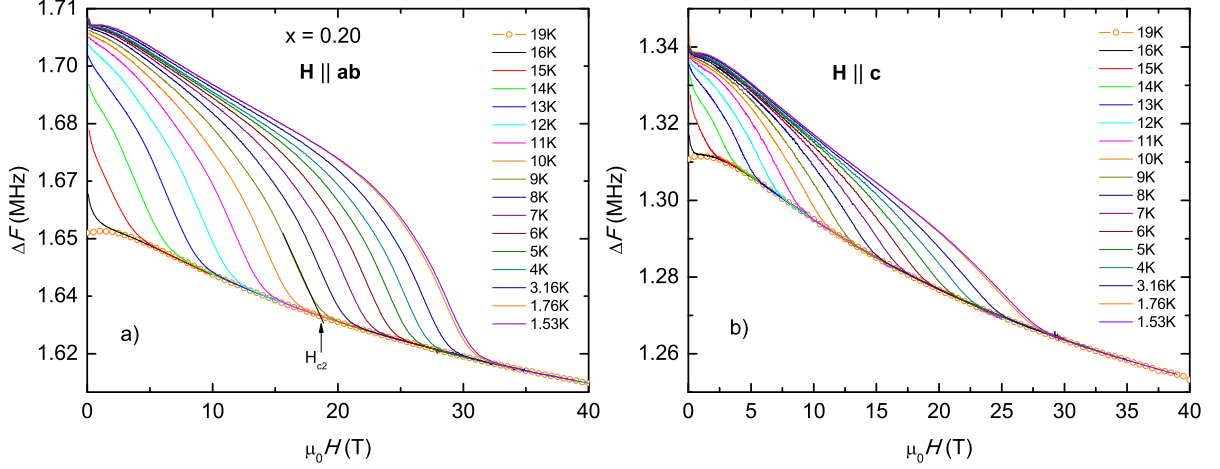


FIG. 2: Frequency shift ( $\Delta F$ ) as a function of magnetic field for  $H \parallel ab$  and  $H \parallel c$  for Eu20 sample at selected temperatures. Open symbols are  $\Delta F$  taken at 19 K as a normal state, background signal. Solid line in (a) shows the criterion used to determine  $H_{c2}(T)$ .

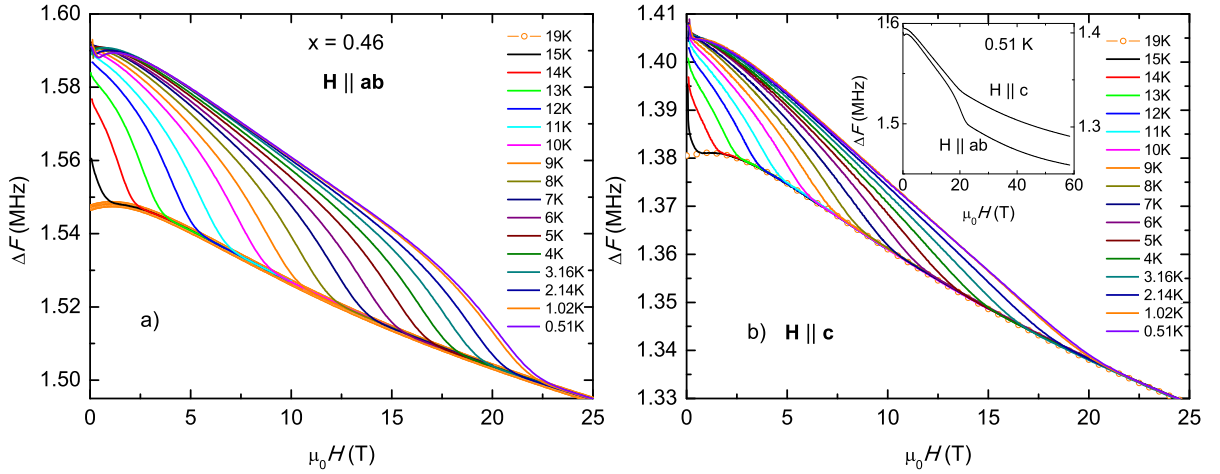


FIG. 3:  $\Delta F$  as a function of magnetic field for  $H \parallel ab$  and  $H \parallel c$  for Eu46. Inset in (b) shows the measurements up to 60 T at the base temperature of 0.51 K.

compensate the exchange field or the exchange field has the same sign as the external field and no cancellation is realized.

Figure 4 shows the  $H_{c2}(T)$  curves for  $H \parallel ab$  ( $H_{c2}^{ab}$ ) and  $H \parallel c$  ( $H_{c2}^c$ ) for both samples. For the Eu20 sample,  $H_{c2}^{ab}(T)$  is almost linear close to  $T_c$ , a traditional Werthamer-Helfand-Hohenberg (WHH) behavior, but  $H_{c2}^c(T)$  exhibits a significant upward curvature. This negative curvature is even more pronounced for the Eu46 sample in Fig. 4(b) for both field orientations. The dashed lines in Fig. 4 are fits to the conventional one-band WHH theory.<sup>21</sup> The  $H_{c2}(T)$  values from direct measurements are far above the prediction of WHH theory, except for the  $H \parallel ab$  curve of Eu20 sample (see later

discussion). The other mechanism for limiting  $H_{c2}(T)$  is the Pauli spin paramagnetic effect as a result of Zeeman effect exceeding the condensation energy of Copper pairs, given by  $\mu_0 H_p = 1.84 T_c$  for isotropic s-wave pairing in the weak coupling limit.<sup>22</sup>  $\mu_0 H_p$  is estimated to be 30.9 T and 29.4 T for Eu20 and Eu46 respectively. These values are close to the experimental results extrapolated to 0 K, implying that the Pauli paramagnetic effect might be the dominant pair breaking mechanism for limiting the upper critical fields in these compounds. It is worth noting that for the  $x = 0.46$  sample the magnitude of  $H_{c2}(T)$  is reduced and its curvature is changed. This is not unexpected given the rough doubling of local moment bearing  $\text{Eu}^{2+}$  which manifests very non-linear  $M(H)$  behavior.<sup>12</sup>

TABLE I: Parameters of the fits to the two-band model for  $\text{Sr}_x\text{Eu}_x(\text{Fe}_{0.89}\text{Co}_{0.11})_2\text{As}_2$ 

$x$	$\begin{pmatrix} D_1^{ab} & D_1^c \\ D_2^{ab} & D_2^c \end{pmatrix} (cm^2/s)$	$\begin{pmatrix} \lambda_{11} & \lambda_{12} \\ \lambda_{21} & \lambda_{22} \end{pmatrix}$	$\mu_0 H_{c2}^{ab}(0) (T)$	$\mu_0 H_{c2}^c(0) (T)$	$\xi^{ab}(0) (nm)$	$\xi^c(0) (nm)$
0.20	$\begin{pmatrix} 0.16 & 1.35 \\ 0.36 & 0.15 \end{pmatrix}$	$\begin{pmatrix} 0.19 & 0.194 \\ 0.194 & 0.21 \end{pmatrix}$	31.6	30.4	3.3	3.2
0.46	$\begin{pmatrix} 0.79 & 2.27 \\ 0.28 & 0.25 \end{pmatrix}$	$\begin{pmatrix} 0.2 & 0.082 \\ 0.082 & 0.2 \end{pmatrix}$	22.4	20.4	4.0	3.7

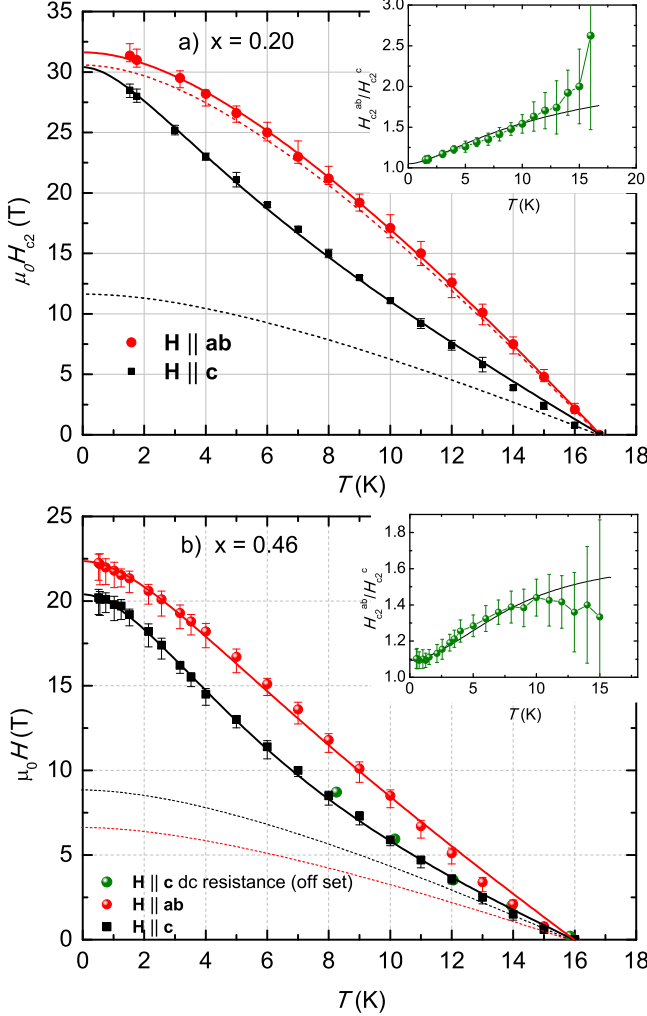


FIG. 4: Anisotropic  $H_{c2}(T)$  for Eu20 and Eu46 single crystals. The green circles in (b) are obtained from the resistivity measurement, in excellent agreement with the pulsed field rf shift measurement. The dotted lines are fits to WHH formula. The solid lines are fits to the two-band model. Insets show the temperature dependence of the anisotropy  $\gamma = H_{c2}^{ab}/H_{c2}^c$  and the solid lines are the calculated curve of the two-band model fits.

Anomalous upward curvature of  $H_{c2}(T)$  has been observed in other multiband systems like  $\text{MgB}_2$ <sup>23</sup> and recently in FeAs superconductors e.g.  $\text{Ba}(\text{Fe}_{0.9}\text{Co}_{0.1})_2\text{As}_2$ <sup>5</sup>,  $\text{LaFeAsO}_{0.89}\text{F}_{0.11}$ <sup>8</sup>,  $\text{NdFeAsO}_{0.7}\text{F}_{0.3}$ <sup>9</sup> and  $\text{Sr}(\text{Fe}_{0.9}\text{Co}_{0.1})_2\text{As}_2$  thin film<sup>10</sup> and explained within a two-band BCS model by taking into account the inter and intra band scattering in  $H_{c2}(T)$ .<sup>23</sup> In the two-band s-wave theory, the intra and interband interactions are described by a  $2 \times 2$  matrix of the BCS coupling constants  $\lambda_{mn}$ , for which  $\lambda_{11}$  and  $\lambda_{22}$  quantify the intraband coupling and  $\lambda_{12}$  and  $\lambda_{21}$  describe interband coupling.  $H_{c2}(T)$  is described by a parametric equation<sup>23</sup>

$$\ln \frac{T}{T_{c0}} = -(U(h) + U(\frac{D_2}{D_1}h) + \frac{\lambda_0}{w})/2$$

$$+ [(U(h) - U(\frac{D_2}{D_1}h) - \frac{\lambda_-}{w})^2/4 + \frac{\lambda_{12}\lambda_{21}}{w}]^{1/2}$$

$$U(h) = \psi(1/2 + h) - \psi(1/2)$$

$$H_{c2} = 2\phi_0 k_B T h / \hbar D_1$$

where  $\psi(x)$  is the digamma function,  $\phi_0$  is the flux quantum,  $k_B$  is the Boltzmann constant,  $\hbar$  is the Planck constant,  $D_{1,2}$  are the anisotropic diffusivities of each band, for  $H_{c2}^{ab}$  the diffusivity  $D_1$  should be replaced by  $(D_1^{ab}D_1^c)^{1/2}$ ,  $\lambda_- = \lambda_{11} - \lambda_{22}$ ,  $\lambda_0 = (\lambda_-^2 + 4\lambda_{12}\lambda_{21})^{1/2}$ ,  $w = \lambda_{11}\lambda_{22} - \lambda_{12}\lambda_{21}$ . Since only the product of  $\lambda_{12}$  and  $\lambda_{21}$  appears in the equation, we can assume  $\lambda_{12} = \lambda_{21}$ . The fits to both  $H_{c2}^{ab}(T)$  and  $H_{c2}^c(T)$  for each sample are performed simultaneously in a self-consistent manner. The model fits the data remarkably well, it captures the main features of the  $H_{c2}(T)$  curves. The fitting parameters are listed in Table I. In terms of diffusivity, the two bands exhibit strong asymmetry, i.e. the diffusivity ratio  $\sqrt{D_2^{ab}D_2^c}/\sqrt{D_1^{ab}D_1^c} \sim 0.5$  and  $0.2$  for Eu20 and Eu46 respectively. Thus superconductivity results from an anisotropic band with high diffusivity and a more isotropic band with smaller diffusivity. It should be noted that for the Eu20 sample  $H_{c2}^c(T)$  shows negative curvature whereas  $H_{c2}^{ab}(T)$  shows behavior similar to that conforms with the conventional WHH theory. The two types of curvature for different field orientations have also been observed in  $\text{Ba}(\text{Fe}_{0.93}\text{Co}_{0.07})_2\text{As}_2$ .<sup>24</sup> But here we are describing both of them within the two-band model. For equal diffusivities of the two bands, i.e.  $\eta = D_2/D_1 = 1$ , the parametric equation of above reduces to the one-gang de-Gennes-Maki formula in WHH



theory,  $\ln t + U(h) = 0$ .<sup>23</sup> The diffusivity ratio of the Eu20 sample,  $\eta^{ab} = D_2^{ab}/(D_1^{ab}D_1^c)^{1/2}$  and  $\eta^c = D_2^c/D_1^c$ , is 0.77 and 0.11 for  $H \parallel ab$  and  $H \parallel c$  respectively. Therefore it is reasonable to expect  $H_{c2}^{ab}(T)$  with near unity  $\eta$  to show WHH-like behavior in contrast to  $H_{c2}^c(T)$  with much lower  $\eta$  to be two-band-like.

The Eu20 sample shows strong interband pairing, i.e.  $\lambda_{12}\lambda_{21} \simeq \lambda_{11}\lambda_{22}$ , whereas the two bands become more non-interacting in the Eu46 sample, as indicated by  $\lambda_{12}\lambda_{21} \ll \lambda_{11}\lambda_{22}$ . It is noteworthy that the intraband pairing strength,  $\lambda_{11}$  and  $\lambda_{22}$ , remains almost unchanged for Eu concentration increases from 0.20 to 0.46, only the interband coupling decreases, with  $T_c$  decreases slowly from 16.8 K to 16 K. This observation may imply that superconductivity could be dominated by the intraband pairing and not particularly sensitive to disorder and interband scattering. With the fitted values of  $H_{c2}(T)$  at 0 K, we can estimate the anisotropic coherence length using  $\xi^{ab} = \sqrt{\phi_0/2\pi H_{c2}^c}$  and  $\xi^c = \phi_0/2\pi\xi^{ab}H_{c2}^{ab}$  (Table I). Both  $\xi^{ab}$  and  $\xi^c$  are much larger than the spacing between the superconducting FeAs layers ( $\sim 6\text{\AA}$ ) in  $\text{Sr}_{1-x}\text{Eu}_x(\text{Fe}_{0.89}\text{Co}_{0.11})_2\text{As}_2$ , suggesting a 3D characteristic of superconductivity.

The anisotropy of  $H_{c2}(T)$  is plotted in the insets of Fig. 4. Both  $\gamma$  decrease with decreasing temperature and approach 1 at zero temperature. It is qualitatively similar to that of the  $\text{LiFeAs}$ <sup>6</sup>,  $(\text{Ba,K})\text{Fe}_2\text{As}_2$ <sup>4,11</sup> and  $\text{LaFeAsO}_{0.89}\text{F}_{0.11}$ .<sup>8</sup> The isotropy of  $H_{c2}(T)$  in FeAs superconductors with different carrier dopings is unexpected since distinctive hole and electron Fermi surfaces may be responsible for superconductivity with different dopings. For our Eu20 and Eu46 samples, there could be two factors contributing to the decreasing anisotropy: i) at low temperature, band 2 with lower band anisotropy  $D_2^{ab}/D_2^c \sim 2.4 - 1.1$  may become more important than band 1 with  $D_1^{ab}/D_1^c \sim 0.12 - 0.35$ ; ii) the two bands have opposing anisotropy of diffusivity, for band 1,  $(D_1^{ab}/D_1^c) < 1$ , whereas for band 2,  $(D_2^{ab}/D_2^c) > 1$ . The calculated  $\gamma$  from the fits are shown as the solid lines in the insets. They well reproduce the temperature dependence of  $\gamma$  within error bars. Aside from the two-band model, another way of understanding the low temperature approach to isotropy is by invoking Pauli limit as upper limit for both directions.

#### IV. CONCLUSIONS

To summarize, we measured the anisotropic  $H_{c2}(T)$  for single crystals of  $\text{Sr}_{1-x}\text{Eu}_x(\text{Fe}_{0.89}\text{Co}_{0.11})_2\text{As}_2$  ( $x = 0.20$  and  $0.46$ ). Despite the presence of  $\text{Eu}^{2+}$  moment, the Jaccarino-Peter effect is not observed up to 60 T at base temperature of 0.5 K, it may be intrinsically absent in this system or higher applied magnetic field may be needed.  $H_{c2}(T)$  deviates from the WHH behavior as manifested by the upward curvature and is probably limited by Pauli paramagnetic pair breaking. The temperature dependence of  $H_{c2}(T)$  is well described by a model

of two bands with opposing anisotropy and large diffusivity difference. The  $H_{c2}(T)$  becomes more isotropic at low temperature.

#### ACKNOWLEDGMENTS

This work was carried out at the Iowa State University and supported by the AFOSR-MURI grant #FA9550-09-1-0603 (R. H. and P. C. C.). Part of this work was performed at Ames Laboratory, US DOE, under contract # DE-AC02-07CH 11358 (S. L. B. and P. C. C.). S. L. B. was also partially supported by the State of Iowa through the Iowa State University. Work at the NHMFL is supported by the NSF, the DOE and the State of Florida.

\*Present address: Center for Nanophysics & Advanced Materials and Department of Physics, University of Maryland, College Park MD 20742-4111, USA.

†Present address: Department of physics, Mu'tah University, Mu'tah, Karak, 61710, Jordan.

- 
- <sup>1</sup> M. Shahbazi, X. L. Wang, C. Shekhar, O. N. Srivastava, Z. W. Lin, J. G. Zhu, and S. X. Dou
  - <sup>2</sup> C. Senatore, R. Flukiger, M. Cantoni, G. Wu, R. H. Liu, and X. H. Chen, *Phys. Rev. B* 78, 054514 (2008)
  - <sup>3</sup> Xiaolin Wang, Shaban Reza Ghorbani, Germanas Peleckis, Shixue Dou, *Adv. Mater.* 21, 236 (2009)
  - <sup>4</sup> M. M. Altarawneh, K. Collar, and C. H. Mielke, N. Ni, S. L. Bud'ko, and P. C. Canfield, *Phys. Rev. B* 78, 220505(R) (2008)
  - <sup>5</sup> Mika Kano, Yoshimitsu Kohama, David Graf, Fedor Balakirev, Athena S. Sefat, Michael A. McGuire, Brian C. Sales, David Mandrus, and Stanley W. Tozer, *J. Phys. Soc. Jpn.* 78, 084719 (2009)
  - <sup>6</sup> J. L. Zhang, L. Jiao, F. F. Balakirev, X. C. Wang, C. Q. Jin, H. Q. Yuan, *Phys. Rev. B* 83, 174506 (2011)
  - <sup>7</sup> N. Ni, S. L. Bud'ko, A. Kreyssig, S. Nandi, G. E. Rustan, A. I. Goldman, S. Gupta, J. D. Corbett, A. Kracher, and P. C. Canfield, *Phys. Rev. B* 78, 014507 (2008)
  - <sup>8</sup> F. Hunte, J. Jaroszynski, A. Gurevich, D. C. Larbalestier, R. Jin, A. S. Sefat, M. A. McGuire, B. C. Sales, D. K. Christen & D. Mandrus, *Nature* 453, 903 (2008)
  - <sup>9</sup> J. Jaroszynski, F. Hunte, L. Balicas, Youn-jung Jo, I. Raicevic, A. Gurevich, D. C. Larbalestier, F. F. Balakirev, L. Fang, P. Cheng, Y. Jia, and H. H. Wen, *Phys. Rev. B* 78, 174523 (2008)
  - <sup>10</sup> S. A. Baily, Y. Kohama, H. Hiramatsu, B. Maiorov, F. F. Balakirev, M. Hirano, and H. Hosono, *Phys. Rev. Lett.* 102, 117004 (2009)
  - <sup>11</sup> H. Q. Yuan, J. S. Singleton, F. F. Balakirev, S. A. Baily, G. F. Chen, J. L. Luo, and N. L. Wang, *Nature* 457, 565 (2009)
  - <sup>12</sup> Rongwei Hu, Sergey L. Bud'ko, Warren E. Straszheim, Paul C. Canfield, *Phys. Rev. B* 83, 094520 (2011)
  - <sup>13</sup> V. Jaccarino and M. Peter, *Phys. Rev. Lett.* 9, 290 (1962)
  - <sup>14</sup> Ø Fischer, M. Decroux, S. Roth, R. Chevrel and M. Sergent, *J. Phys. C: Solid State Phys.*, 8, 474 (1975)
  - <sup>15</sup> H. W. Meul, C. Rossel, M. Decroux, and Ø Fischer, G. Remenyi, A. Briggs, *Phys. Rev. Lett.* 53, 497–500 (1984)
  - <sup>16</sup> C. Mielke, J. Singleton, M.-S. Nam, N. Harrison, C. C. Agosta, B. Fravel, and L. K. Montgomery, *J. Phys.: Condens. Matter* 13, 8325 (2001)
  - <sup>17</sup> T. Coffey, Z. Bayindir, J. F. DeCarolis, M. Bennett, G. Esper, and C. C. Agosta, *Rev. Sci. Instrum.* 71, 4600 (2000)
  - <sup>18</sup> M. M. Altarawneh, C. H. Mielke, and J. S. Brooks, *Rev. Sci. Instrum.* 80, 066104 (2009)
  - <sup>19</sup> Amikam Aharoni, *J. Appl. Phys.* 83, 3432 (1998)
  - <sup>20</sup> E. D. Mun, M. M. Altarawneh, C. H. Mielke, and V. S. Zapf, R. Hu, S. L. Bud'ko, and P. C. Canfield, *Phys. Rev. B* 83, 100514(R) (2011)
  - <sup>21</sup> N. R. Werthamer, E. Helfand, P. C. Hohenberg, *Phys. Rev.* 147, 295 (1966)
  - <sup>22</sup> A. M. Clogston, *Phys. Rev. Lett.* 9, 266 (1962)
  - <sup>23</sup> A. Gurevich, *Phys. Rev. B* 67, 184515 (2003)
  - <sup>24</sup> V. A. Gasparov, L. Drigo, A. Audouard, D. L. Sun, C. T. Lin, S. L. Bud'ko, P. C. Canfield, F. Wolff-Fabris and J. Wosnitza, *JETP Letters*, 93, 667 (2011)